

This is the submitted version of the article:

Szydzik C., Gavela A.F., Herranz S., Roccisano J., Knoerzer M., Thurgood P., Khoshmanesh K., Mitchell A., Lechuga L.M.. An automated optofluidic biosensor platform combining interferometric sensors and injection moulded microfluidics. *Lab on a Chip*, (2017). 17. : 2793 - . 10.1039/c7lc00524e.

Available at: <https://dx.doi.org/10.1039/c7lc00524e>



An automated optofluidic biosensor platform combining interferometric sensors and injection moulded microfluidics

Journal:	<i>Lab on a Chip</i>
Manuscript ID	LC-ART-05-2017-000524
Article Type:	Paper
Date Submitted by the Author:	16-May-2017
Complete List of Authors:	<p>Szydzik, Crispin; RMIT University, School of Electrical and Computer Engineering Gavela, Adrián ; Catalan Institute of Nanoscience and Nanotechnology (ICN2), Nanobiosensors and Bioanalytical Applications Group. Herranz, Sonia; Catalan Institute of Nanoscience and Nanotechnology (ICN2), Nanobiosensors and Bioanalytical Applications Group. Roccisano, Joseph; RMIT University, School of Electrical and Computer Engineering Knoerzer, Markus; RMIT University, School of Engineering Thurgood, Peter; RMIT University, School of Electrical and Computer Engineering Khoshmanesh, Khashayar; RMIT University, School of Engineering Mitchell, Arnan; RMIT University, School of Electrical and Computer Engineering Lechuga, Laura; Catalan Institute of Nanoscience and Nanotechnology (ICN2),</p>

Article type: Full paper

Lab on a Chip



Website www.rsc.org/loc

Impact factor* 5.586

Journal mission To provide a unique forum for the publication of significant and original work related to miniaturisation, at the micro- and nano-scale, of interest to a multidisciplinary readership. The journal seeks to publish work at the interface between physical technological advancements and high impact applications that are of direct interest to a broad audience.

Visit the [LOC website](#) for additional details of the journal scope and expectations.

Article type: Full paper Original scientific work that has not been published previously. These must represent a significant development in the particular field, and are judged according to originality, quality of scientific content and contribution to existing knowledge. Full papers do not have a page limit and should be appropriate in length for scientific content.

Please consider these high standards when making your recommendation to accept or reject. It is essential that all articles submitted to *Lab on a Chip* meet the significant novelty criteria; Lack of novelty is sufficient reason for rejection.

Reviewer responsibilities

Visit the [Reviewer responsibilities website](#) for additional details of the reviewing policy and procedure for Royal Society of Chemistry journals.

When preparing your report, please:

- Use the [journal scope and expectations](#) to assess the manuscript's suitability for publication in *LOC*.
- Comment on the originality, importance, impact and reliability of the science. English language and grammatical errors do not need to be discussed in detail, except where it impedes scientific understanding.
- State clearly whether you think the paper should be accepted or rejected, giving detailed comments that will both help the Editor to make a decision on the paper and the authors to improve it;
- Inform the Editor if there is a conflict of interest, a significant part of the work you cannot review with confidence or if parts of the work have previously been published.
- Provide your report rapidly and within the specified deadline, or inform the Editor immediately if you cannot do so

You can submit your report at <https://mc.manuscriptcentral.com/lc>

The online service for Royal Society of Chemistry authors and reviewers can be found at <http://mc.manuscriptcentral.com/rsc>

Thank you for evaluating this manuscript, your advice as a reviewer for *LOC* is greatly appreciated. To acknowledge this, the Royal Society of Chemistry offers a **25% discount** on our books: <http://www.rsc.org/Shop/books/discounts.asp>.

We hope you will consider submitting your next manuscript to *Lab on a Chip*.

Best wishes,

Dr Sam Keltie
Executive Editor
Royal Society of Chemistry

Professor Abraham Lee
Editor-in-Chief
University of California, Irvine, USA

Barcelona, 12 May 2017

Dear Prof. Lee,

We would like to submit our work titled **“An automated optofluidic biosensor platform combining interferometric sensors and injection moulded microfluidics”** to be considered for publication as an article in *Lab-on-a-chip*.

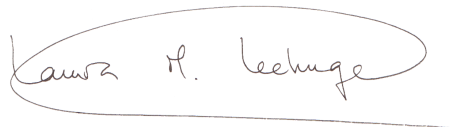
This manuscript describes our recent work on an automated fluid handling module designed for nanophotonic biosensors. This work describes an automated on-chip fluid handling module designed to meet the complex fluidic handling requirements of photonic biosensors, while maintaining compatibility with low-cost, practical and scalable fabrication techniques.

As a proof-of-concept, the module is integrated with a Bimodal Waveguide Interferometric biosensor, and automated to perform a competitive immunoassay for the detection of the antibiotic Tetracycline.

This work represents a major advancement in the development of practical photonic biosensors for real applications, and provides a facilitating platform that could pave the way for automated point-of-care implementation for this specific type of highly sensitive photonic biosensor.

Please do not hesitate to contact us, if you require any further information.

Yours sincerely,



Prof. Laura M. Lechuga



Lab on a Chip

PAPER

An automated optofluidic biosensor platform combining interferometric sensors and injection moulded microfluidics

C. Szydzik^a, A.F. Gavela^b, S. Herranz^b, J. Roccisano^a, M. Knoerzer^a, P. Thurgood^a, K. Khoshmanesh^a, A. Mitchell^a, L.M. Lechuga^{*b}

Received 00th January 20xx,
Accepted 00th January 20xx

DOI: 10.1039/x0xx00000x

www.rsc.org/

A primary limitation preventing practical implementation of photonic biosensors within point-of-care platforms is their integration with fluidic automation subsystems. For most diagnostic applications, photonic biosensors require complex fluid handling protocols; this is especially prominent in the case of competitive immunoassays, commonly used for detection of low-concentration, low-molecular weight biomarkers. For this reason, complex automated microfluidic systems are needed to realise the full point-of-care potential of photonic biosensors. To fulfil this requirement, we propose an on-chip valve-based microfluidic automation module, capable of automating such complex fluid handling. This module is realised through application of a PDMS injection moulding fabrication technique, recently described in our previous work, which enables practical fabrication of normally closed pneumatically actuated elastomeric valves. In this work, these valves are configured to achieve multiplexed reagent addressing for an on-chip diaphragm pump, providing the sample and reagent processing capabilities required for automation of cyclic competitive immunoassays. Application of this technique simplifies fabrication and introduces the potential for mass production, bringing point-of-care integration of complex automated microfluidics into the realm of practicality. This module is integrated with a highly sensitive, label-free Bimodal Waveguide photonic biosensor, and is demonstrated in the context of a proof-of-concept biosensing assay, detecting the low-molecular weight antibiotic Tetracycline.

Introduction

Photonic biosensors enable cost-effective, highly sensitive, and selective label-free detection of target biomarkers¹⁻³, they require relatively simple support equipment and software to operate and a minimal physical footprint⁴. With appropriate functionalisation strategies, these biosensors can be reused multiple times⁵ and have been shown to be capable of exceedingly low limits of detection^{6, 7}. While photonic biosensors are among the most highly sensitive biosensor technologies available², many of their other unique characteristics are highly attractive for point-of-care applications, in which devices are generally required to be compact, self-sufficient and simple to operate while maintaining reliability, accuracy and reproducibility⁸. Despite these advantages, several challenges exist restricting practical adoption of photonic biosensors for point-of-care devices¹. One of the most significant challenges is fluid handling, as photonic biosensors generally require complex flow handling protocols,

with sequential application of multiple reagents and a critical need for fluidic isolation. Fluid handling becomes increasingly complex when advanced assays are required, such as competitive immunoassays, commonly applied when the target analyte to be detected is of low molecular weight and is present in very low concentrations, as is the case with pesticides, toxins or antibiotic residues for food control and environmental monitoring applications⁹⁻¹¹.

The field of microfluidics has been proposed extensively as a solution for point-of-care diagnostic devices for the healthcare sector⁸, and has attracted significant interest in recent years¹²⁻¹⁵. Microfluidic systems intended for point-of-care application must employ simple, ideally automated operational principles, and must maintain compatibility with scalable fabrication techniques suited to mass fabrication^{8, 13}. As a result, few of the fluid handling strategies commonly employed in point-of-care devices are suited to the specific requirements of photonic biosensors, lacking the necessary dynamic functionality, fluid isolation performance and scalability. Further, although integration of photonic biosensors with complex automated microfluidic systems could provide the level of precise fluid handling required for point-of-care, merging of these two technologies is currently challenging due to fabrication complexity, and control of the interfaces necessary for the fluid handling protocols required to operate such sensors.

Numerous complex microfluidic fluid manipulation technologies exist in the literature capable of achieving on-chip

^a School of Engineering, RMIT University, Melbourne Australia.

^b Nanobiosensors and Bioanalytical Applications Group. Catalan Institute of Nanoscience and Nanotechnology (ICN2). CSIC, CIBER-BBN and The Barcelona Institute of Science and Technology, Campus UAB, Bellaterra, 08193 Barcelona, Spain.

*Corresponding author: Laura.lechuga@icn2.cat

Electronic Supplementary Information (ESI) available: (details of any supplementary information available should be included here). See DOI: 10.1039/x0xx00000x

fluidic isolation. Digital microfluidics¹⁶, droplet based microfluidics¹⁷ and pneumatic valve based microfluidic systems¹⁸ are some of the common technologies employed to manipulate, isolate and mix precise volumes of fluid on-chip. Among these technologies, pneumatic valve based microfluidic systems demonstrate the highest potential for flexible and scalable integrated platforms. Microfluidic automation of exceedingly complex fluid handling protocols has been achieved utilising pneumatic valve based systems for numerous applications¹⁸, including lab-on-a-chip platforms¹⁹⁻²¹, and biosensors^{22,23}. Of particular interest, this technology has been applied to fluidic automation of photonic biosensors²⁴⁻²⁶. While application of such automated microfluidic systems provides the required fluidic isolation, a high degree of flexibility, and on-chip fluidic control in a manner not otherwise possible, fabrication of the valves required to operate such devices is generally cumbersome, and integration can become difficult to the point of impracticality.

We have recently begun to explore the possibility for complex integrated microfluidics and integrated optics²⁷. We present here an automated fluid handling module designed for nanophotonic biosensors with complex valved microfluidics realised utilising a simple one-step injection moulding technique²⁸, which can achieve complicated valved microfluidics which significantly reduce fabrication complexity and have the potential for scale-up mass manufacture. We demonstrate the utility of this microfluidic by integrating it with a highly sensitive Bimodal Waveguide photonic biosensor⁴, and demonstrate the functionality of the complete integrated system by performing repeated automated competitive immunoassays for the detection of an analyte of small molecular weight (the antibiotic tetracycline). The ability to realise such high quality valved microfluidics while maintaining simplicity and scalability renders complex automated microfluidics of the sort required for photonic biosensors practical. This work thus represents a major advancement in the development of practical photonic biosensors for point-of-care applications.

Photonic Background

This work harnesses the bimodal waveguide photonic biosensor⁴ (BiMW) depicted in Fig. 1, a photonic interferometric sensor design which has demonstrated excellent biosensing capacities for the detection of diverse biomarkers²⁹⁻³¹. Operation of this sensor is described in detail in previous publications⁴, but for reference a brief description is provided here. In these biosensors, monochromatic visible light is coupled into the photonic chip through a single mode input waveguide (fundamental mode), this mode is then split between two guided modes (fundamental and the first order mode), with the same polarization, through an interface with a step junction in the waveguide geometry. The surface of the biosensor is passivated with the exception of a sensing window, which is functionalised with a specific bioreceptor. Both modes are propagating along the sensing area and their evanescent fields interact with the biomolecules at the waveguide surface. The

evanescent fundamental mode penetrates less deeply into the sensing area, and can thus be used as the reference. Any change in the refractive index of the sensing area causes an interference pattern and in turn, a variation of the intensity distribution of the light exiting at the device output. By measuring the output light intensity distribution, the sensor response can be determined.

Fabrication of the Bimodal waveguide photonic biosensor is achieved in a cleanroom facility using standard microelectronics techniques as outlined in⁴, silicon nitride is used in the fabrication of visible wavelength waveguides, with a silicon dioxide cladding layer. The bimodal waveguide is 3 μm in width, has a rib of 1.5 to 3 nm and a thickness of 150 nm (single mode zone) and 340 nm (bimodal zone). The active photonic area of the chip surface is limited to the photonic sensing window etched into the cladding within the bimodal segment of the waveguide, with an area of 15 mm by 50 μm . Multiple devices are fabricated at wafer level, and later divided into individual chips containing 20 BiMW sensors each, separated by 250 μm . Photonic access is achieved through end-fire coupling on the end of the device while output light is collected with a multi-channel photodiode or CCD camera on the other end.

The sensor surface is functionalised through immobilisation of a specific target, and thus, the selective biomolecular recognition which takes place results in a change of the refractive index at the sensor surface, which perturbs the evanescent field and can thereby be detected as changes in the interferometer output.

Microfluidic subsystem integration

Microfluidic design considerations

As described above, a primary issue hindering development of point-of-care photonic biosensor platforms is practical integration with on-chip microfluidic systems, providing automated sample and reagent fluid handling. Photonic biosensors generally require fairly complex fluid handling protocols, with multiple fluids manipulated sequentially; in addition, fluidic isolation is required in order to eliminate cross

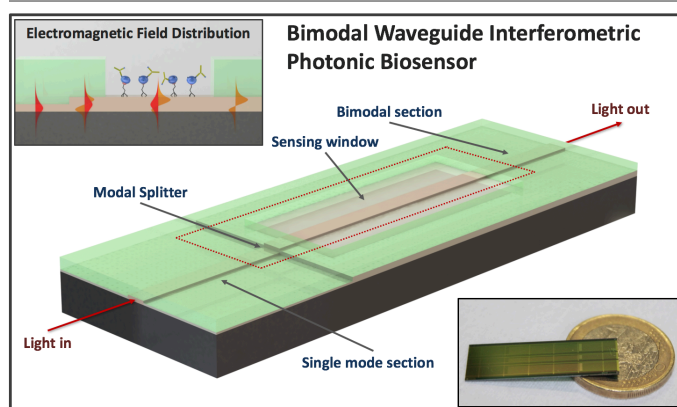


Fig. 1. Scheme illustrating the working principle of a bimodal waveguide biosensor, showing the main components of the Bimodal Waveguide photonic biosensor; inset top left shows how the electromagnetic field associated with the light beam propagates through the waveguide, while the bottom right inset is a photograph of the chip, shown with a 1-Euro coin for reference.

contamination between reagents, and flow conditions must be reproducible. Sample volume is ideally kept to a minimum, with channel geometry minimised in order to ensure an adequate mass transport to the sensor surface to avoid unnecessary delays in the biointeraction. In addition, for practical point-of-care applications, any integrated fluidic system must be cheap to manufacture, with simple interfaces and ideally utilise simple and scalable fabrication techniques compatible with mass production.

Our previous work has primarily utilised simple microfluidic systems fabricated using polydimethylsiloxane (PDMS)⁴, a biocompatible material commonly used in the fabrication of microfluidic devices³². Fluidic isolation was achieved externally through manual valve manipulation, and samples were manually introduced to a sample loop and flushed through the tubing using a syringe pump.

While numerous on-chip fluidic actuation technologies exist in literature, valve based approaches are the best suited to providing fluidic isolation. Due to recent improvements in fabrication techniques²⁸, it should be possible to adapt

normally closed pneumatically driven on-chip valve based technologies²³ to realise a sufficiently complex, but reliable, valved microfluidic system to automate a photonic BiMW biosensor.

Microfluidic system overview

Fig 2 presents a diagram of the fluid handling module proposed for automatic operation of the BiMW sensor. Microfluidic channels are patterned into either side of a thin PDMS slab seen in **Fig.2A**, utilising an injection moulding fabrication technique. This slab is bonded with a thicker PDMS interface slab, biopsy punched with interfaces and reservoirs of appropriate diameter as seen in **Fig.2B**. The PDMS chip is then placed over the BiMW sensor and its associated photonic interface and thermal stage, and clamped in place as outlined in⁴. The module includes several gate valves to control the flow of the various fluids required for biosensing assays. These gate valves are multiplexed to minimise the number of external pneumatic actuators required. The module also includes a single on-chip diaphragm pump to actuate each of the fluids as selected by the

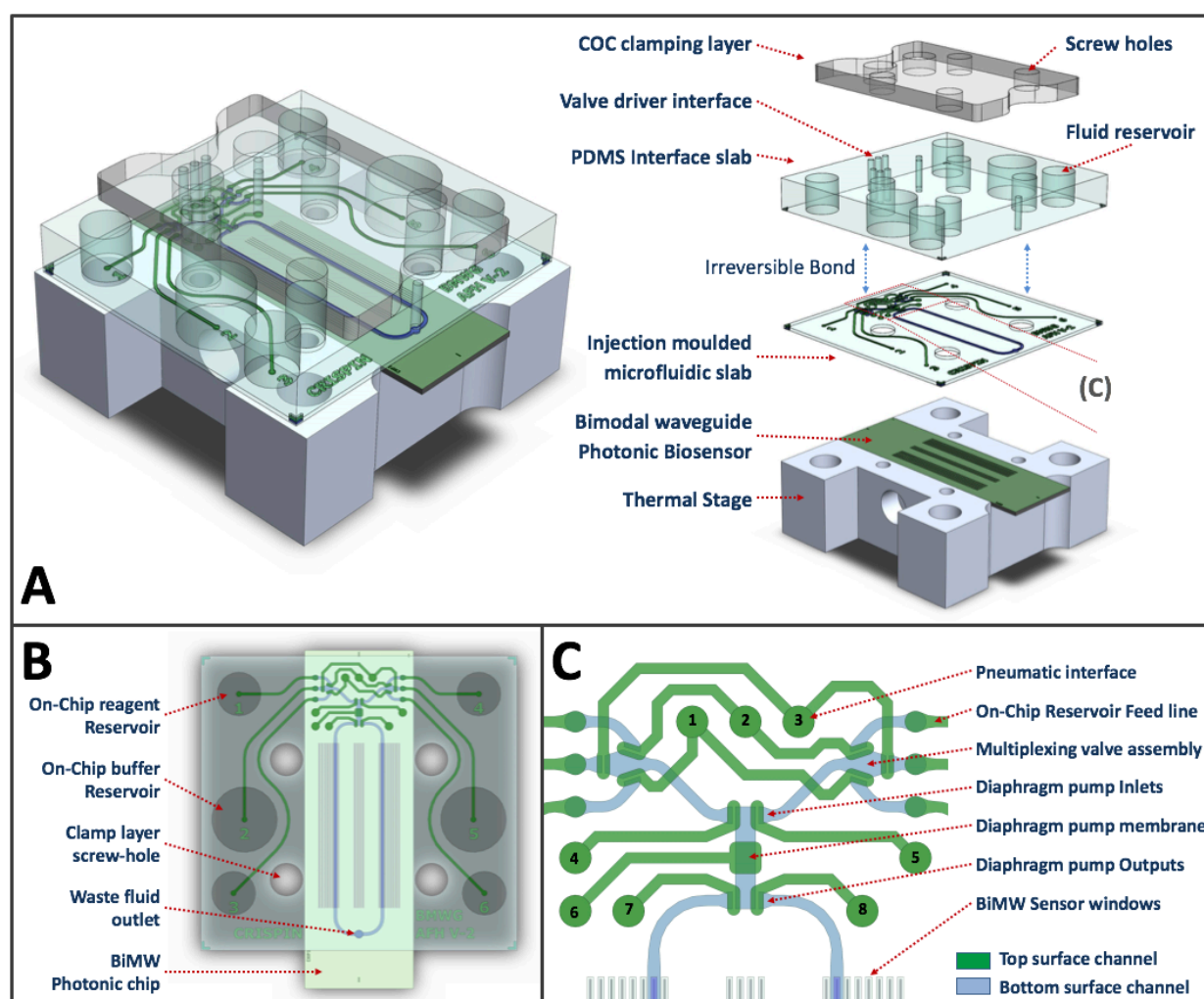


Fig.2. Schematic of the automated microfluidic module and its various components. **Fig.2A** shows a CAD model of the reusable microfluidic module reversibly bonded to the BiMW sensor with a clamp structure, which is fixed to the thermal stage of the setup with screws. Right is an exploded view showing the two primary components, a PDMS interface slab irreversibly bonded to a double sided injection moulded PDMS slab, and a clamping layer. **Fig.2B** highlights locations of the primary fluidic reservoirs and overall alignment of the microfluidic and the photonic sensor, while **Fig.2C** shows an enlarged schematic of the various active microfluidic components, with features on the top surface of the injection moulded PDMS slab shown in green and the bottom layer shown in blue.

gate valve assemblies. All fluidic channels patterned into the module are 250 μm wide, with exception of valve, pump and viaduct structures. The top channels, shown as green in **Fig. 2** are 160 μm deep, while all primary fluidic channels patterned on the bottom of the slab, and shown in blue, are 140 μm deep. 6 on-chip Fluidic reservoirs, accessible through routing channels in the top layer, are interfaced through 500 μm biopsy punched viaducts from the top to bottom layer. Further detail on functional sub-units is presented below.

Normally closed pneumatically actuated gate valves

The normally closed pneumatically actuated gate valves are illustrated in **Fig. 2C**. At the centre of each valve is a gate structure, a barrier of PDMS, 400 μm long and 100 μm wide, these gates are normally lowered to close channels, and can be pneumatically lifted to open the channel. This gate is patterned as a protrusion on a thin elastic membrane (60 - 100 μm thick) which can be deformed. Above this membrane is an oval shaped open channel which acts as an actuation chamber, with a width of 350 μm , length of 750 μm and channel depth of 160 μm . When this chamber is evacuated, the elastomeric PDMS membrane deforms upward, lifting the gate from the bottom of the channel, creating an opening in the barrier and allowing flow across the valve gate. Positive pressure is used to actively and rapidly close the valve gates, and is critical to enabling rapid valve switching, required for efficient pumping. In order to actuate and automate all on-chip valves, a customised external support equipment and software package was developed. This valve driver system operates on a similar principal to those shown in various pneumatically driven on-chip valve systems³³. The driver system interfaces with a control computer, and utilises micro-solenoid valves (Burkert Type 6650-189292) to switch external pneumatic valves between two reservoirs, maintained at user defined pressure with an automated pressure regulation sub-system. A Python script is used to rapidly switch individual solenoid valves in sequences appropriate to operation of on-chip control components.

Multiplexing valve assemblies

Fluidic multiplexing is required to minimize the number of active valve control lines, and thereby to minimise external support equipment. It should be possible to achieve multiplexing, while reducing the chance of fluidic contamination due to dead volume in fluidic junctions, through minimisation of valve size and by optimising valve and channel geometry. Multiplexing is achieved using parallel valve assemblies as shown in **Fig. 2C**. These assemblies consist of three gate valves, controlling the flow through channels that connect with the on-chip fluid reservoirs. These valves are operated symmetrically, with each of the valves paired with a complementary valve on the opposite assembly. Each assembly is addressed with its corresponding valve on the pump, such that only one of the open pairs is aspirated during pump actuation. These assemblies are designed with an elongated hexagonal geometry, with valve gates placed in a triangular configuration, minimising the distance between valve actuation chambers and minimising fluidic dead volume within the

assembly. Running buffer reservoirs feed into the central gate, facilitating washout of the assembly when switching between reservoirs.

On-chip diaphragm pump

On-chip fluid propulsion is a critical function required to achieve automation; valve based on-chip pump systems generally utilise peristaltic principles to achieve this³⁴. With the availability of the previously described gate valves, it is possible to also consider a pneumatically driven diaphragm pump for fluid actuation with active control of gate valves around this diaphragm, to control the direction of fluid flow. The on-chip pump consists of a symmetrical chamber structure with two inlets, two outlets, and a flexible diaphragm, illustrated in **Fig. 2C** while utilisation of a dedicated membrane, using an 800 μm square actuation chamber, provides propulsion. The desired inlet is initially opened, and the diaphragm is lifted, increasing the volume of the pump chamber and drawing fluid from the inlet; the inlet is then closed, the desired outlet opened, and the diaphragm is forced closed, distending into the pump chamber and reducing its volume, forcing the contained fluid through the open outlet.

Valve assemblies are positioned as close as possible to the pump structure, so as to reduce fluidic volume of the connecting channel, minimising required reagent volume and assay times. Due to the paired actuation of the valve assemblies, diffusion of fluids across open valve gates can contaminate the fluid within the unused assembly. To avoid this and ensure pure sample or reagent delivery to the sensor surface, it is necessary to purge the volume of the assembly to waste when switching between ports on opposite assemblies. This, as well as priming of all fluidic lines, is done through the waste channel output of the pump.

Microfluidic Fabrication

Fabrication of the microfluidic modules was accomplished utilising a combination of the 'membrane sandwich' approach³⁵, and a novel PDMS Injection moulding technique, previously described by our group²⁸. In brief, complementary mould structures are fabricated using standard photolithography techniques or 3D printing. All fluidic channel structures to be in contact with the sensor surface are patterned onto a bottom mould, while all actuation channels and via or interconnecting channels are patterned onto a complementary top mould. Polydimethylsiloxane (PDMS) pre-polymer (Sylgard 184 Silicone Elastomer - Dow Corning) is mixed with curing agent with a weight ratio of 10:1 respectively, and thoroughly degassed under vacuum. Degassed Pre-Polymer composite is then introduced between aligned complementary mould structures. The assembled mould structure is then placed into an oven for 1 hour at 80°C, when cured, the mould structures are separated and the PDMS slab (shown in **Fig. 2A**) is extracted. A blank PDMS interface slab of approximately 4-5 mm thickness is then biopsy punched with appropriately aligned pneumatic interface holes (0.75 mm) and on-chip fluidic reservoirs (4-6 mm). The actuation side of the injection moulded PDMS slab is irreversibly

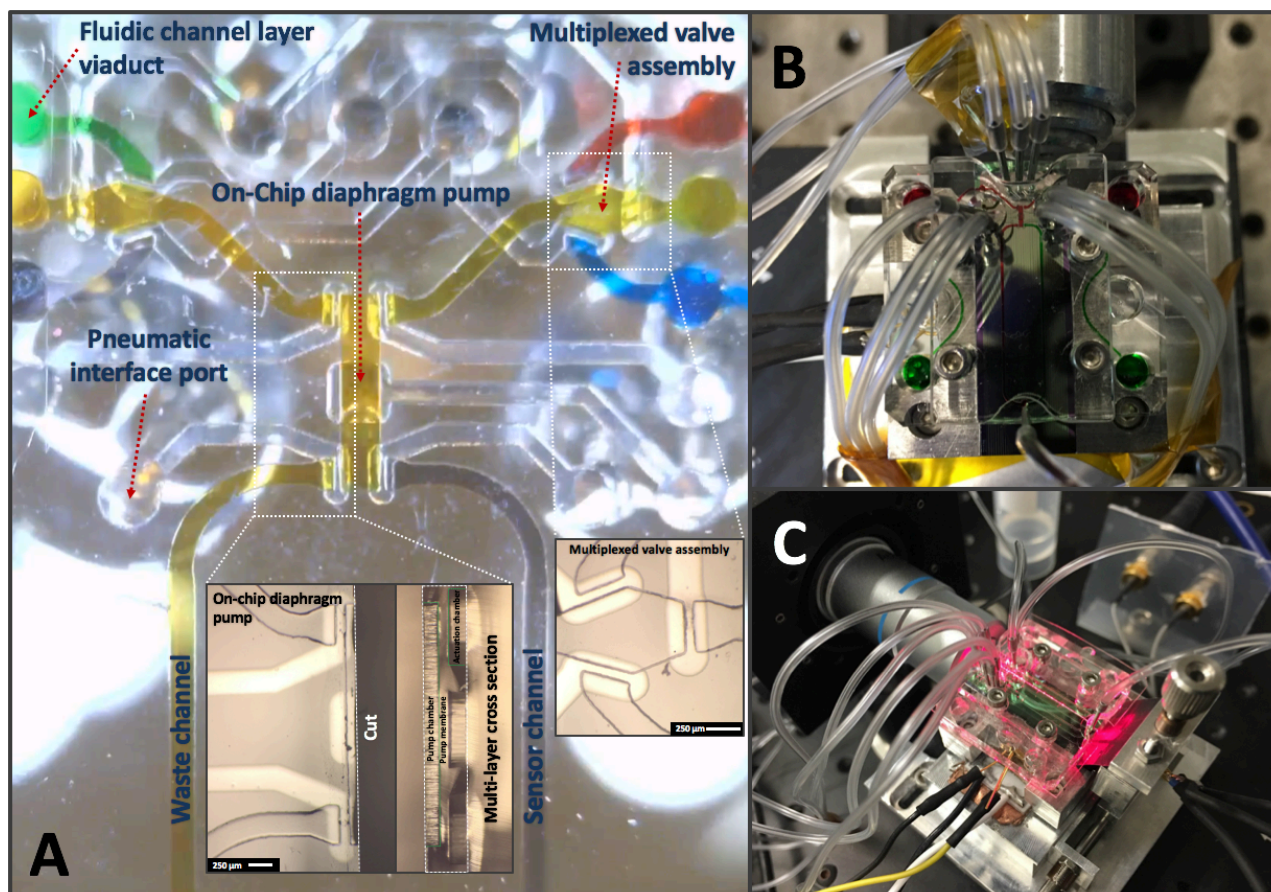


Fig. 3. Imaging of the microfluidic subsystems., **Fig.3A** shows a low-resolution microscopy image of the area illustrated in **Fig.2C** imaged in operation with color dyes while bonded to a glass slide. Control components are labeled, with high resolution images of the multiplexing valve assembly and pump inset including cross sectional cut of the pump structure. **Fig.3B** shows integration of the microfluidic module with the BiMW sensor, with channels highlighted with color dyes, while **Fig.3C** shows an operational image of the module integrated with an active BiMW sensor.

plasma bonded to the interface slab; this assembled PDMS module can then be aligned over the sensor surface of the BiMW sensor and reversibly bonded. A thin (250–500 μm) PDMS cap can then be placed over the top of the module, this layer has cut-outs allowing access for pneumatic interface tubing, it is reversibly bonded and prevents evaporation of fluid from the on-chip reservoirs. The thin evaporation preventative layer can easily be lifted at the edge of the assembly to allow access to the on-chip reservoirs; small perforations can be made with a hypodermic needle in the areas centred on these reservoirs, these perforations will seal due to the elastomeric nature of the PDMS as long as the PDMS is flat, however they allow gas transfer when a pressure differential is applied, equilibrating pressure within the reservoirs. Finally, the assembled module is clamped using screws between a polymethyl methacrylate (PMMA) clamp layer and the BiMW setup outlined in ⁴. The physically realised PDMS device is presented in **Fig. 3**.

Microfluidic subsystem characterisation

To verify functionality of the microfluidic control systems, each of the components was initially verified independently. **Fig3A–B** shows these subsystems in operation with food dyes verifying fluidic isolation, while the final integrated configuration is shown in **Fig.3C**. Low resolution microscopy of the entire module in operation with food dyes illustrates the functionality

of the multiplexing valve assemblies and pump in **Fig.3A**, where the running buffer is represented with yellow dye in central reservoirs, while other colours represent reagent and sample fluids, respectively. Supplementary video-1 demonstrates operation of the on-chip pump with food dyes purged through the waste channel. Inset within **Fig.3A** includes higher resolution images of the pump and multiplexing assembly structures, as well as a cross-sectional cut of the pump structure, showing relative thickness of the valve structural layers. This dissected valve geometry is explored in further detail in Supplementary Fig.S-1. **Fig.3B** shows the microfluidic module aligned and reversibly bonded with a BiMW sensor chip, assessing valve functionality and verifying fluidic isolation. **3C** shows the module integrated with an active BiMW photonic sensor while in operation. The on-chip diaphragm pump was experimentally demonstrated to achieve stable flow rates up to approximately $7.5 \mu\text{L min}^{-1}$. During Automated experimental protocols flow rates of $1.5 \mu\text{L min}^{-1}$ and $6 \mu\text{L min}^{-1}$ were used for sample flow and waste purging operations respectively.

Biosensing proof-of-concept

In order to assess the functionality of the microfluidic module interfaced with the BiMW sensor, we have employed fluidic automation in the context of a complex competitive biosensing

assay requiring repetitive reference and competitive analysis cycles.

As a proof-of-concept we demonstrate the detection of the antibiotic Tetracycline. Tetracycline is one of the most widely used antibiotics, exhibiting a broad spectrum of antimicrobial activity against a variety of disease-producing bacteria. Antibiotics are used extensively in human and veterinary medicine, and also in aquaculture, in order to prevent or treat microbial infections. Antibiotic residues from different sources (household, pharmaceutical industry, and hospital) enter into municipal sewage but they are only partially eliminated at sewage treatment plants and as consequence, residues of these drugs and their metabolites are released into the environment. The uncontrolled exposure to antibiotic residues increases the appearance of antibiotic-resistant bacteria, which represents a serious and growing human health threat worldwide, because infections from resistant bacteria are increasingly difficult and expensive to treat. Therefore, due to its widespread use, monitoring of tetracycline levels is important in numerous fields such as clinical diagnosis³⁶, food processing³⁷, and environmental pollutant monitoring¹⁰. Tetracycline has a low molecular weight (444.45) and is normally found in very low concentrations, for these reasons competitive immunoassays are well suited for its detection. In a competitive immunoassay format the chemical target to be detected, present in a sample, competes for the antibody binding sites with a receptor previously attached to the sensor surface. The sample containing the chemical target to be detected is incubated for a few minutes with a fixed quantity of the corresponding antibody and then flowed on to the sensor surface. The signal is obtained by the interaction of the remaining free antibody of the incubated solution (sample+antibody) with the receptor layer. Therefore, the signal is inversely proportional to the concentration of the chemical target in the sample. The bioreceptor layer is expected to be re-usable during various analysis cycles by regeneration of the sensor surface, i.e. by dissociating the receptor-antibody interaction without destroying the bioreceptor activity.

It should be possible to automate our developed integrated microfluidic-BiMW system to perform the complex and repetitive fluid handling required for the competitive assay in order to detect the presence of tetracycline. Automation of this integrated system should allow a significant increase in assay repeatability, while reducing manual labour as well as the influence of any associated manual error variables.

In these experiments we have employed a tetracycline conjugate (DoxAc10-AD) and an antiserum specific for the family of tetracycline-related antibiotics (As256). The suitability of this immuno-reagents pair was first tested by a standard Surface Plasmon Resonance (SPR) Biosensor (*data not shown*), achieving a LOD of 0.09 nM and an IC₅₀ value of 3.6 nM. The SPR sensor could be reused for several measure-regeneration cycles of tetracycline by using 10 mM NaOH solution as a regeneration buffer.

Surface Biofunctionalisation and competitive immunoassay

A previous surface biofunctionalisation of the sensor surface is mandatory to perform the analysis. In this case we have employed a silanisation protocol with carboxyethylsilanetriol sodium salt (CTES) which provides a surface functionalized with carboxyl groups, allowing the further covalent immobilisation of bioreceptors presenting amino groups in their structure, such as the evaluated hapten-protein conjugate (DoxAc10-AD) by the well-known EDC/NHS chemistry. Briefly, the BiMW sensors were first thoroughly cleaned, oxidised (oxygen plasma treatment, 5 min) and immersed in an aqueous 0.5% CTES solution for 1 h. After that, the CTES-treated chips were rinsed with deionised water, dried under nitrogen stream and thermally cured at 110° C for 1 h. CTES silanisation is performed utilising previously optimised protocols by our Group⁵. The silanised chip is then aligned with the microfluidic module such that a BiMW sensing window is located within the sensor channel, and reversibly bonded. The assembled device is then placed into the experimental setup and connected to the valve driver support equipment (for further information see: Supplementary Material SM-1: Experimental setup). Further surface functionalisation steps are performed utilising the automated microfluidic module, at a flow rate of 1.5 μL min⁻¹, an automated on-chip fluid handling protocol is executed with minimal user input, thereby reducing user introduced variability and resulting in more reproducible surface conditions. Due to the reactive and time critical nature of functionalisation reagents, it is necessary to prepare and load reagents sequentially into on-chip reservoirs as they are required. MilliQ DI water is used as a running buffer for the following process: initially, the reactive carboxylic groups of the silanised sensor surface are activated by flowing 200 mM EDC/ 50 mM sulfo-NHS solution in 100 mM MES buffer containing 0.5 M NaCl, at pH 5.0 for 10 minutes. The surface is briefly cleansed with DI water, followed by flow of the receptor molecule (DoxAc10-AD) at a concentration of 20 μg/mL in SA buffer (pH 5) allowing bonding with the freshly activated surface for 15 minutes. An additional DI water rinse is followed by a final flow of Ethanolamine 1M (pH 8.5), to deactivate residual carboxylic groups and to remove electrostatically bound ligand in an effort to avoid non-specific adsorptions. At this stage the sensor assembly is ready for the competitive assay. In a competitive immunoassay different steps are involved. Initially, the sensor surface needs to be conditioned with a buffer solution, until reaching a stable baseline signal. Then, the sample is mixed with a constant concentration of the antibody and the mixture is injected onto the sensor surface, allowing the interaction between the free antibody and the receptor immobilised onto the surface. The sensor surface is then washed with buffer to remove all unbound material and the signal after stabilisation is evaluated. Finally, the surface is regenerated and conditioned again with buffer, starting a new measurement cycle.

The surface functionalisation protocol and the competitive immunoassay employed are briefly introduced in Fig. 4. Fig. 4A illustrates the sensor surface in its initial state, 4B-D illustrate the technique used to immobilise the receptor (DoxAc10-AD) described above. Fig. 4E illustrates a functionalised surface in which the receptor molecule has captured the specific antibody;

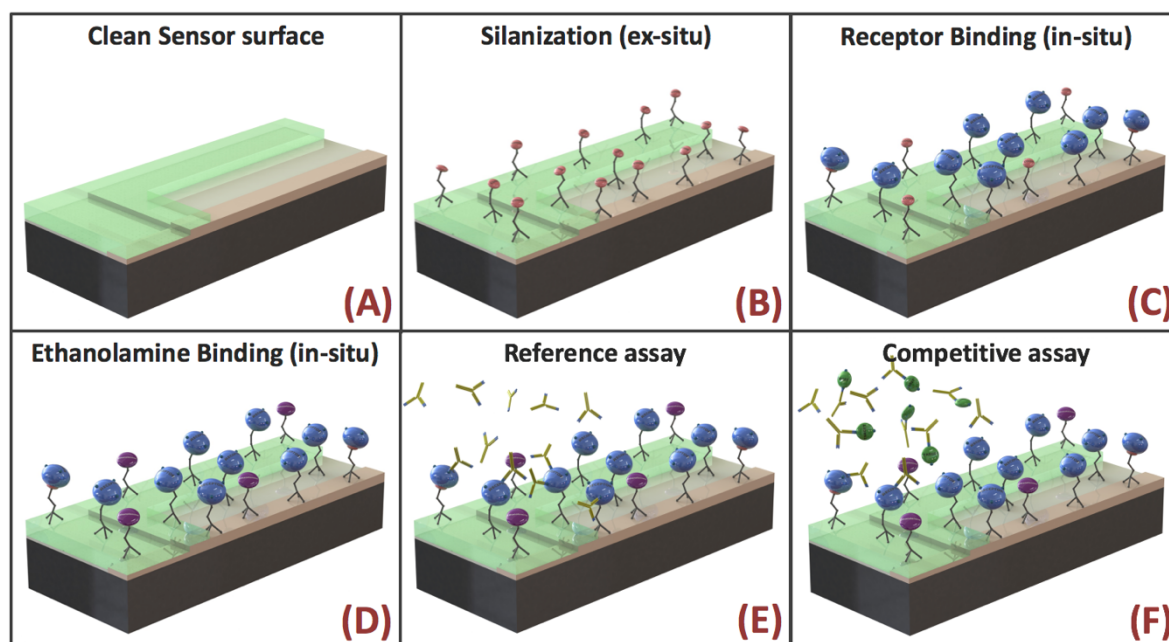


Fig. 4. Conceptually illustrated surface conditions during surface biofunctionalisation and during a competitive assay. **Fig. 4A** shows a clean sensor surface prior to functionalisation, this image represents a cross section of the BiMW, showing the waveguide surface (foreground) at the sensor window area with the passivation layer seen in green. **Fig. 4B** illustrates the sensor surface post silanisation with CTES, **C** illustrates receptor binding, followed by ethanolamine treatment in **D**, blocking any unbound carboxylic groups. **Fig. 4E** illustrates surface interactions during a reference assay, with antibodies binding to the receptor molecules, while **F** illustrates a competitive assay, antibody binding sites are occupied by target molecules reducing overall surface interaction.

following this **Fig. 4F**. shows the target-antibody interactions blocking antibodies from surface interaction.

Automated assay protocol

In order to perform a competitive immunoassay, the automated system must be able to perform an initial reference assay in order to benchmark sensor response to a known antibody concentration, followed by a competitive assay which will be used to quantify the target concentration. This 'cycle' of reference and competitive assays are complementary and must be repeated for each competitive assay. Each assay requires an initial flow of buffer solution in order to achieve a sensor baseline; this is followed by a sample flow, allowing surface interaction, likewise followed by a secondary flow of buffer as a sample washout step. The secondary baseline attained at washout can then be compared with initial baseline magnitude to interpret the effect of surface interaction. The sensor surface finally requires regeneration by actively stripping the bound antibodies using a mild acid or basic conditions, and a final buffer flow applied to bring the system back to a ready state. Automation of these assay protocols, implemented using the microfluidic module developed in this work, should result in time consistent cycling of the required steps of the complex assay, reducing interaction time variability and ensuring pure sample and reagent delivery. In order to achieve this, 20-minute detection cycles are programmed using Python script, automating all fluid handling required to perform an assay and subsequent surface regeneration using the BiMW sensor, with the exception of sample preparation. Initially running buffer, Phosphate buffered saline (PBS) and regeneration fluid (NaOH-10mM), are loaded into the on-chip reservoirs. An automated

protocol then primes these channels, sending a small volume through the waste outlet, ensuring any bubbles are purged from the system and ensuring reagents are ready at the valve gate when required. Following initial priming, sample can be loaded and the automated sequence initiated, this sequence will initially flush sample through the waste path, cleansing the system and ensuring that sample delivered to the sensor is bubble and contaminant free; the sample is then directed through the sensor channel for 10 minutes passing a total sample volume of approximately 15 μ L, during which time specific target binding can occur. Following this surface interaction period, the system flows PBS over the sensor for 4 minutes to flush out any unbound sample and to obtain a secondary baseline, this is followed by a 3-minute regeneration cycle where NaOH is directed over the sensor surface, stripping bound antibodies and readying the system for subsequent detection cycles; finally, the sensor surface is washed out with PBS for an additional 3 minutes returning the system to a ready state for subsequent measurements.

This automated protocol performs the assay fluid handling consistently, ensuring that flow conditions and interaction times are consistent for each assay. This was initially verified through manipulation of colour food dyes in place of sample and reagent fluids, as shown in **Fig. 3C**, prior to the assay application.

Biosensing of tetracycline antibiotic

Application of the automated assay protocol to perform fluid handling required for the competitive assay should allow repeated reproducible assay cycles, allowing target biomarker quantification, and evaluation of surface chemistry and its

effectiveness following multiple regeneration cycles. Prior to experimentation, the sensor was initially biofunctionalised, reagents loaded into on-chip reservoirs and channels primed using an automated priming protocol. Then, the response of the sensor was evaluated by using the automated assay protocol.

As proof of concept, two different samples were analysed: PBS (sample free of antibiotic, used as a reference sample) and a 2 nM tetracycline solution in PBS. First, the sample was mixed with the antibody (AS-256) to a final concentration of 1 $\mu\text{g}/\text{mL}$. Then, 15 μL of the sample-antibody mixture was passed over the sensor over 10 minutes. During this step, the free antibodies interact with the receptor immobilized onto the sensor surface. It is expected that the presence of tetracycline in the sample will result in a lower interaction signal than the reference

(competitive assay). During these experiments, the reference assay (sample free of tetracycline) was repeated before each competitive assay (2 nM tetracycline sample), in an attempt to compensate for degradation of the sensor surface occurring as a result of repeated surface regeneration.

Fig.5 shows the sensor response for a sample free of tetracycline (reference assay) and a sample containing tetracycline in a concentration of 2 nM (competitive assay), sequentially analysed. **Fig.5A** shows sensor readings during an example 20-minute automated measurement cycle running a target-free reference sample, with inset (1-4) conceptually illustrating interactions occurring on the surface of the sensor at various times during the cycle. The reference sample is mixed with the antibody and pipetted into the appropriate reservoir

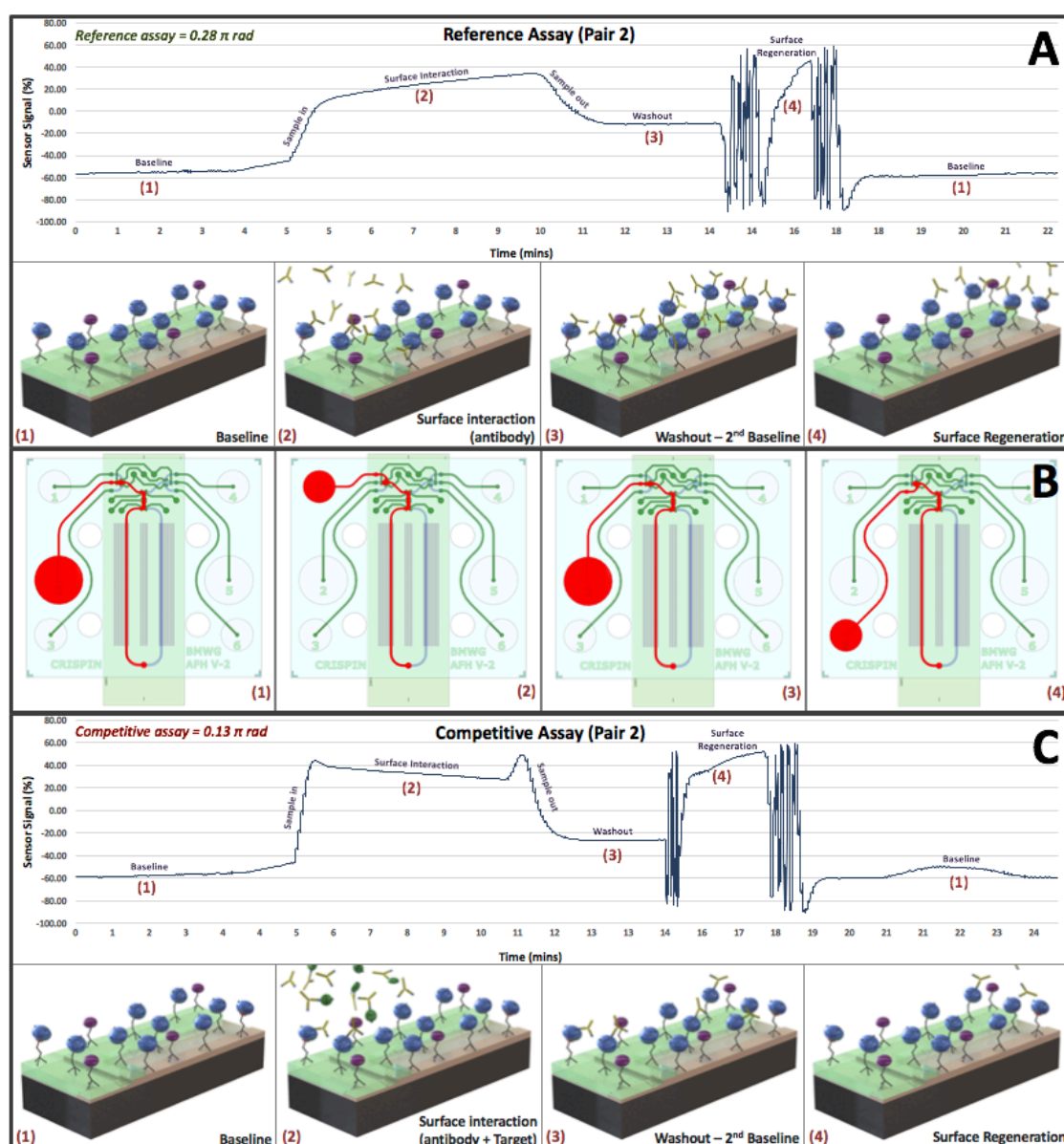


Fig.5. Illustration of the surface interactions occurring at various time points during a reference and competitive assay pair, performed sequentially. **Fig.5A** shows real-time sensor data during an example reference assay, with inset (1-4) conceptually illustrating interactions occurring on the sensor surface at critical time points during the cycle. **Fig.5B** (1-4) highlights the fluidic path taken from the corresponding reservoir at the same time points during the assay, while **Fig.5C** displays sensor readings obtained in a competitive assay performed immediately following the reference assay, along with corresponding conceptual representations of surface interactions in inset **Fig.5C** (1-4).

and the automated detection cycle is initiated. **Fig.5B (1-4)** highlights the fluidic path taken from associated reservoirs at time points corresponding to **5A** and **5C**. Initially the sensor is immersed in PBS at a constant flow-rate of $1.5 \mu\text{L min}^{-1}$; this is allowed to form a stable baseline, **(1)** before introduction of the sample. Initially, introduction of the sample causes a sharp change in signal due to a bulk change in the refractive index of the spiked sample, this is followed by a fixed surface interaction period in which antibodies present in the sample bind to the immobilised receptor, gradually modifying refractive index at the sensor surface, which can be seen as a gradual change in the signal and is conceptually illustrated in **(2)**. Sample washout can be seen as a sharp change, corresponding in magnitude to that observed at sample inflow, this is due to the refractive index of the fluid returning to that of the running buffer or PBS, forming a secondary baseline, shown conceptually in **(3)**. Finally, the surface of the sensor is stripped of bound antibodies using a regeneration solution (NaOH,10mM), this surface regeneration step **(4)** prepares the sensor surface for subsequent detection cycles, following a return to running buffer (PBS) and a return to the initial baseline **(1)**

Surface interactions are quantified by assessing the phase variation of the BiMW interferometer, taking into account that a complete oscillation or fringe corresponds to a 2π rad phase variation. The arbitrary sensor signal (%) value, shown in **Fig.5A** and **C** is tracked from the initial baseline time point in **5A(1)** to the secondary baseline at time point **5A(3)**, taking any transitions across the fringe into account and subtracting the bulk refractive index peak. The total distance travelled represents the magnitude of the surface interaction signal, and are shown relative to π inset in **Fig.5A** and **C**

Fig.5C displays sensor readings obtained during a competitive assay performed immediately following the reference, along with corresponding conceptual representations of surface interactions in insets of **Fig.5C(1-4)**. The competitive assay is performed using the same automated protocol as the reference; however the introduced sample contains 2 nM of Tetracycline. It can be noted that the resultant increase in bulk refractive index due to additional components present in the sample has increased the magnitude of the spike observed at sample introduction and washout. It can be seen that the gradient of the surface interaction shown in area **(2)**, is reduced when compared with the reference sample. It is also clear that the sensor response (overall magnitude of surface interaction, inset in **5A** and **C**) is reduced in the competitive assay due to the presence of the target molecules (tetracycline) in the sample, occupying the binding sites of the antibody, thereby reducing the quantity of available antibodies capable of binding to the receptor in the surface by an amount proportional to the target concentration. **Fig.6A** overlays the response of a 2 nM tetracycline sample (competitive assay) and its corresponding reference. As it can be seen, the presence of 2 nM tetracycline leads to sensor response of 0.13π rad comparing to 0.28π rad for a sample free of antibiotic (reference), i.e. the presence of tetracycline lead to a 54% inhibition of the sensor response. The response of the competitive assay can be expressed as a percentage of its

corresponding reference assay, this is shown in the inset in **Fig.6A**, which corresponds to cycle 2 in **Fig.6B**.

In order to assess the stability of the proof-of-concept surface functionalisation, repetitive reference and competitive cycles were performed, with target and antibody concentrations maintained at constant levels for each repetition. **Fig.6B** illustrates the results, with reference cycles shown in green and competitive assays shown in red. Raw sensor data for each assay is shown in Supplementary Fig.S-2.

As can be observed in figure 6B, the sensor response to reference assays in subsequent pairs reduces significantly. This is most noticeable between the first two assay pairs, and is presumably due to degradation of the immobilized receptor during the regeneration step. As the presence of target analyte is detected as response inhibition, this sensor degradation can introduce a false positive result. For this reason, In order to dynamically compensate for surface degradation and increase the lifetime of the biosensor, each competitive assay was directly preceded by a reference assay. this could be avoided in future work by optimizing the sensor surface functionalisation procedure (receptor immobilization) and regeneration step. Each assay pair was normalized through comparison of the competitive result with its corresponding reference as a percentage, and the competitive signal in % shown in **Fig.6C**.

It can be observed that the response of the sensor to the presence of tetracycline is comparatively stable, with signals (sample/reference ratio) at between 40–50 % for the initial 4 assay pairs, this indicates relative surface stability for at least 8 measurement-regeneration cycles. After 8 analysis a clear sensor degradation is observed, due to the repeated exposure of the bioreceptors to the regeneration solution (basic media). The increase in the competitive signal is presumably due to the increase in non-specific binding events occurring as surface degradation results in the biolayer becoming less specific. This biolayer lifetime is consistent with our previous results³⁰, however it is presumable that improvements to the surface functionalisation protocol used in this proof-of-concept work could significantly improve surface integrity.

Conclusion

This work demonstrates a proof-of-concept implementation of an automated fluid handling module for photonic biosensors. The module is fabricated utilising a one-step injection moulding technique which significantly reduces fabrication complexity of normally closed on-chip elastomer valves. This work makes use of the fabrication technique to realise on-chip fluid handling architecture required for operation of a highly sensitive bimodal waveguide photonic biosensor, automating complex fluid handling protocols required for the operation of a competitive immunoassay.

The capacity of the automated system is demonstrated in a proof of concept competitive immunoassay for the detection of the common antibiotic Tetracycline. The system is shown to perform repetitive automated assay cycles, allowing a high degree of experimental control and temporal resolution. The system demonstrates multiple reference and competitive assay

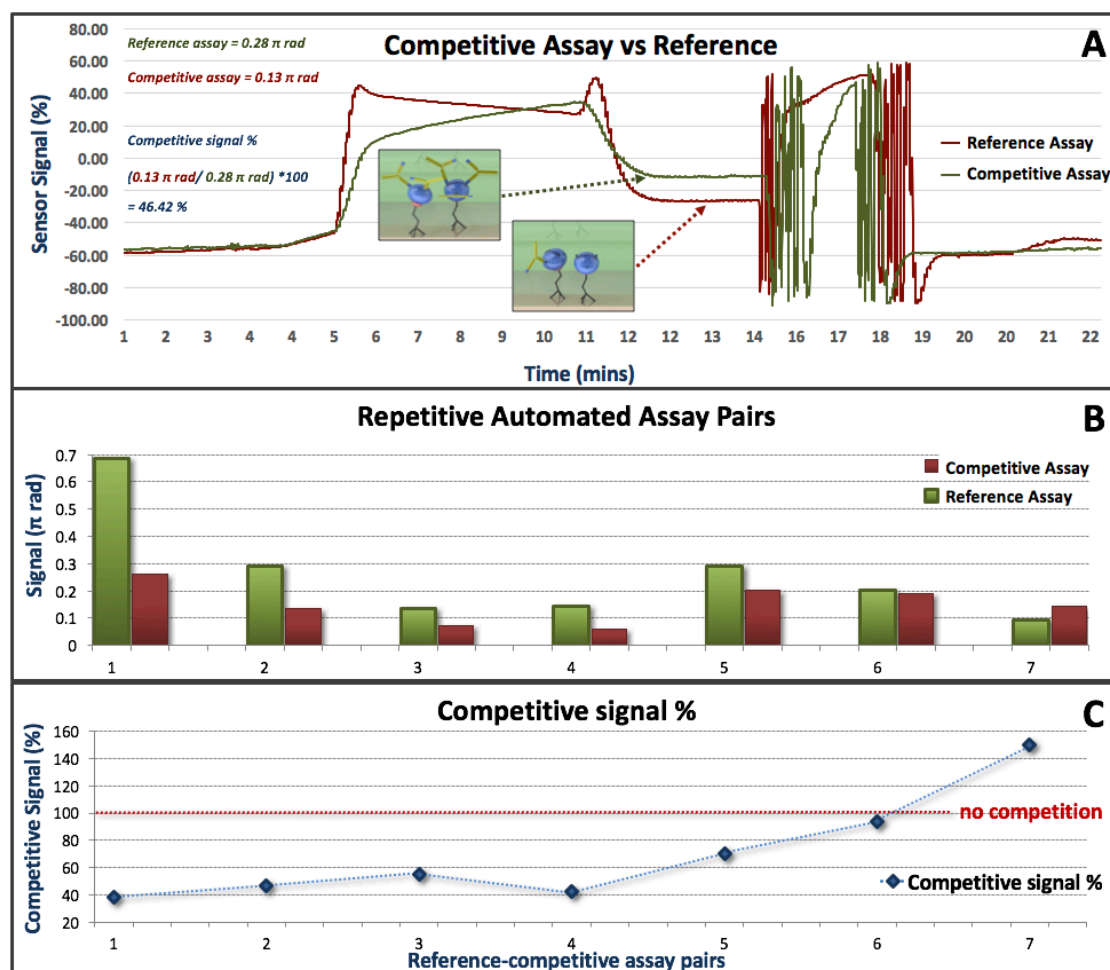


Fig. 6. Signal interpretation and performance of the proof-of-concept functionalized surface during repetitive regeneration cycles with fixed sample concentrations. **Fig. 6A** shows superimposed reference and competitive assay. The presence of tetracycline in the sample leads to an inhibition of the sensor response. **Fig. 6B** shows the sensor response for 14 sequential measurement-regeneration cycles, alternating reference sample (free of antibiotic) and spiked sample (2 nM tetracycline). **Fig. 6C** shows normalised results with each competitive assay as a percentage of its corresponding reference cycle.

cycles, regenerating the sensor bioreceptor later between assays, as would be necessary in real applications requiring periodic testing, such as in food quality control or environmental monitoring.

This research represents a significant advancement in development of practical point-of-care photonic biosensors, providing complex automated fluid handling capabilities compatible with simple and scalable fabrication and robust integration. This research is intended to reduce the cost and effort required for the fabrication of complex lab-on-a-chip platforms, while increasing the level of functional integration, making application of these intricate devices across a broad range of research fields more practical. In addition, a sufficient reduction in fabrication complexity is intended to enable a higher level of fluidic control sophistication in point-of-care medical diagnostic devices, allowing use of more complex biosensors. This research could potentially be integrated into commercial large scale fabrication of point-of-care devices.

The automated nature of this system makes it suited to performing repetitive assay cycles which could be used to sweep parameters in order to optimise surface chemistry. Future work will include optimising the biolayer and

regeneration protocol, with the intention of providing more stable biosensors and increasing sensor lifetime. Further expansion of the system is intended to allow for multiplexing of multiple biosensors, as well as the addition of sample preparation subsystems, providing additional functionality critical to point-of-care applications.

Acknowledgements

C. S. would like to express thanks to benefactors of the Professor Robert and Josephine Shanks Scholarship.

This work has been funded by the 7FP (EU, BRAAVOO Grant Agreement No 614010). The nanoB2A is a consolidated research group (Grup de Recerca) of the Generalitat de Catalunya and has support from the Departament d'Universitats, Recerca i Societat de la Informació de la Generalitat de Catalunya (2014 SGR 624). ICN2 acknowledges support of the Spanish MINECO through the Severo Ochoa Centers of Excellence Program under Grant SEV-2013-0295. This work has made use of the Spanish ICTS Network MICRONANOFABS partially supported by MEINCOM.

References

1. M.-C. Estevez, M. Alvarez and L. M. Lechuga, *Laser & Photonics Reviews* **6** (4), 463-487 (2012).
2. A. Fernández Gavela, D. Grajales García, J. C. Ramirez and L. M. Lechuga, *Sensors* **16** (3), 285 (2016).
3. J. E. Baker, R. Sriram and B. L. Miller, *Lab on a Chip* **17** (9), 1570-1577 (2017).
4. K. E. Zinoviev, A. B. González-Guerrero, C. Domínguez and L. M. Lechuga, *Journal of Lightwave Technology* **29** (13), 1926-1930 (2011).
5. A. B. González-Guerrero, M. Alvarez, A. G. Castaño, C. Domínguez and L. M. Lechuga, *Journal of colloid and interface science* **393**, 402-410 (2013).
6. J.-H. Han, H.-J. Kim, L. Sudheendra, S. J. Gee, B. D. Hammock and I. M. Kennedy, *Analytical chemistry* **85** (6), 3104-3109 (2013).
7. C. S. Huertas, D. Fariña and L. M. Lechuga, *ACS Sensors* **1** (6), 748-756 (2016).
8. W. Jung, J. Han, J.-W. Choi and C. H. Ahn, *Microelectronic Engineering* **132**, 46-57 (2015).
9. J. Adrian, S. Pasche, J.-M. Diserens, F. Sánchez-Baeza, H. Gao, M.-P. Marco and G. Voirin, *Biosensors and Bioelectronics* **24** (11), 3340-3346 (2009).
10. N. Kemper, *Ecological indicators* **8** (1), 1-13 (2008).
11. B. Chocarro-Ruiz, A. Fernández-Gavela, S. Herranz and L. M. Lechuga, *Current Opinion in Biotechnology* **45**, 175-183 (2017).
12. C. D. Chin, V. Linder and S. K. Sia, *Lab on a Chip* **12** (12), 2118-2134 (2012).
13. V. Gubala, L. F. Harris, A. J. Ricco, M. X. Tan and D. E. Williams, *Analytical chemistry* **84** (2), 487-515 (2011).
14. F. B. Myers and L. P. Lee, *Lab on a Chip* **8** (12), 2015-2031 (2008).
15. A. K. Yetisen, M. S. Akram and C. R. Lowe, *Lab on a Chip* **13** (12), 2210-2251 (2013).
16. K. Choi, A. H. Ng, R. Fobel and A. R. Wheeler, *Annual review of analytical chemistry* **5**, 413-440 (2012).
17. S.-Y. Teh, R. Lin, L.-H. Hung and A. P. Lee, *Lab on a Chip* **8** (2), 198-220 (2008).
18. J. Melin and S. R. Quake, *Annu. Rev. Biophys. Biomol. Struct.* **36**, 213-231 (2007).
19. R. Gomez-Sjoeborg, A. A. Leyrat, D. M. Pirone, C. S. Chen and S. R. Quake, *Analytical chemistry* **79** (22), 8557-8563 (2007).
20. L. M. Fidalgo and S. J. Maerkl, *Lab on a Chip* **11** (9), 1612-1619 (2011).
21. Y. C. Yap, T. C. Dickson, A. E. King, M. C. Breadmore and R. M. Guijt, *Biomicrofluidics* **8** (4), 044110 (2014).
22. J. Kim, E. C. Jensen, A. M. Stockton and R. A. Mathies, *Analytical chemistry* **85** (16), 7682-7688 (2013).
23. J. Kim, A. M. Stockton, E. C. Jensen and R. A. Mathies, *Lab on a Chip* **16** (5), 812-819 (2016).
24. H. Cai, J. Parks, T. Wall, M. Stott, A. Stambaugh, K. Alfson, A. Griffiths, R. Mathies, R. Carrion and J. Patterson, *Scientific reports* **5**, 14494-14494 (2014).
25. J. W. Parks, M. A. Olson, J. Kim, D. Ozcelik, H. Cai, R. Carrion Jr, J. Patterson, R. Mathies, A. Hawkins and H. Schmidt, *Biomicrofluidics* **8** (5), 054111 (2014).
26. B. R. Schudel, C. J. Choi, B. T. Cunningham and P. J. Kenis, *Lab on a Chip* **9** (12), 1676-1680 (2009).
27. C. Szydzik, A. F. Gavela, J. Roccisano, S. Herranz, A. Mitchell and L. M. Lechuga, presented at the SPIE BioPhotonics Australasia, 2016 (unpublished).
28. C. Szydzik, B. Niego, G. Dalzell, M. Knoerzer, F. Ball, W. Nesbitt, R. Medcalf, K. Khoshmanesh and A. Mitchell, *RSC Advances* **6** (91), 87988-87994 (2016).
29. C. S. Huertas, S. Domínguez-Zotes and L. M. Lechuga, *Scientific Reports* **7** (2017).
30. J. Maldonado, A. B. González-Guerrero, C. Domínguez and L. M. Lechuga, *Biosensors and Bioelectronics* **85**, 310-316 (2016).
31. A. B. González-Guerrero, J. Maldonado, S. Dante, D. Grajales and L. M. Lechuga, *Journal of Biophotonics* (2016).
32. S. K. Sia and G. M. Whitesides, *Electrophoresis* **24** (21), 3563-3576 (2003).
33. E. C. Jensen, A. M. Stockton, T. N. Chiesl, J. Kim, A. Bera and R. A. Mathies, *Lab on a Chip* **13** (2), 288-296 (2013).
34. W. H. Grover, A. M. Skelley, C. N. Liu, E. T. Lagally and R. A. Mathies, *Sensors and Actuators B: Chemical* **89** (3), 315-323 (2003).
35. J. R. Anderson, D. T. Chiu, R. J. Jackman, O. Cherniavskaya, J. C. McDonald, H. Wu, S. H. Whitesides and G. M. Whitesides, *Analytical chemistry* **72** (14), 3158-3164 (2000).
36. I. Chopra and M. Roberts, *Microbiology and molecular biology reviews* **65** (2), 232-260 (2001).
37. C. Nebot, M. Guarddon, F. Seco, A. Iglesias, J. M. Miranda, C. M. Franco and A. Cepeda, *Food Control* **46**, 495-501 (2014).

Supplementary Material:

An automated optofluidic biosensor platform combining interferometric sensors and injection moulded microfluidics

C. Szydzik¹, A.F. Gavela², S. Herranz², J. Roccisano¹, M. Knoerzer¹, P. Thurgood¹,
K. Khoshmanesh¹, A. Mitchell¹, L.M. Lechuga^{*2}

¹School of Engineering, RMIT University, Melbourne Australia

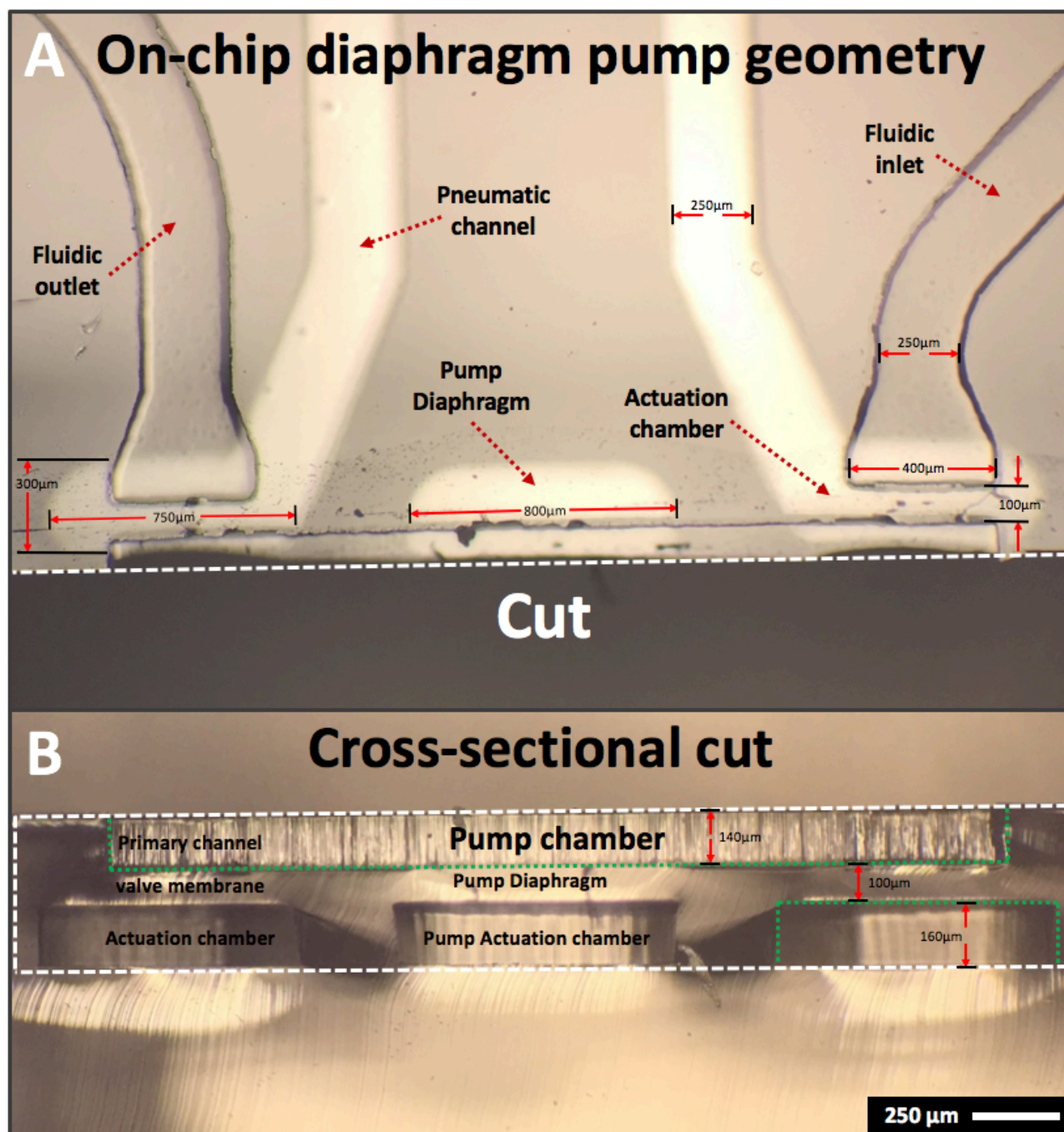
²Nanobiosensors and Bioanalytical Applications Group. Catalan Institute of Nanoscience and Nanotechnology (ICN2). CSIC, CIBER-BBN and The Barcelona Institute of Science and Technology, Campus UAB, Bellaterra, 08193 Barcelona, Spain.

* Corresponding authors:
Laura.lechuga@icn2.cat

Supplementary Material SM-1: Experimental setup

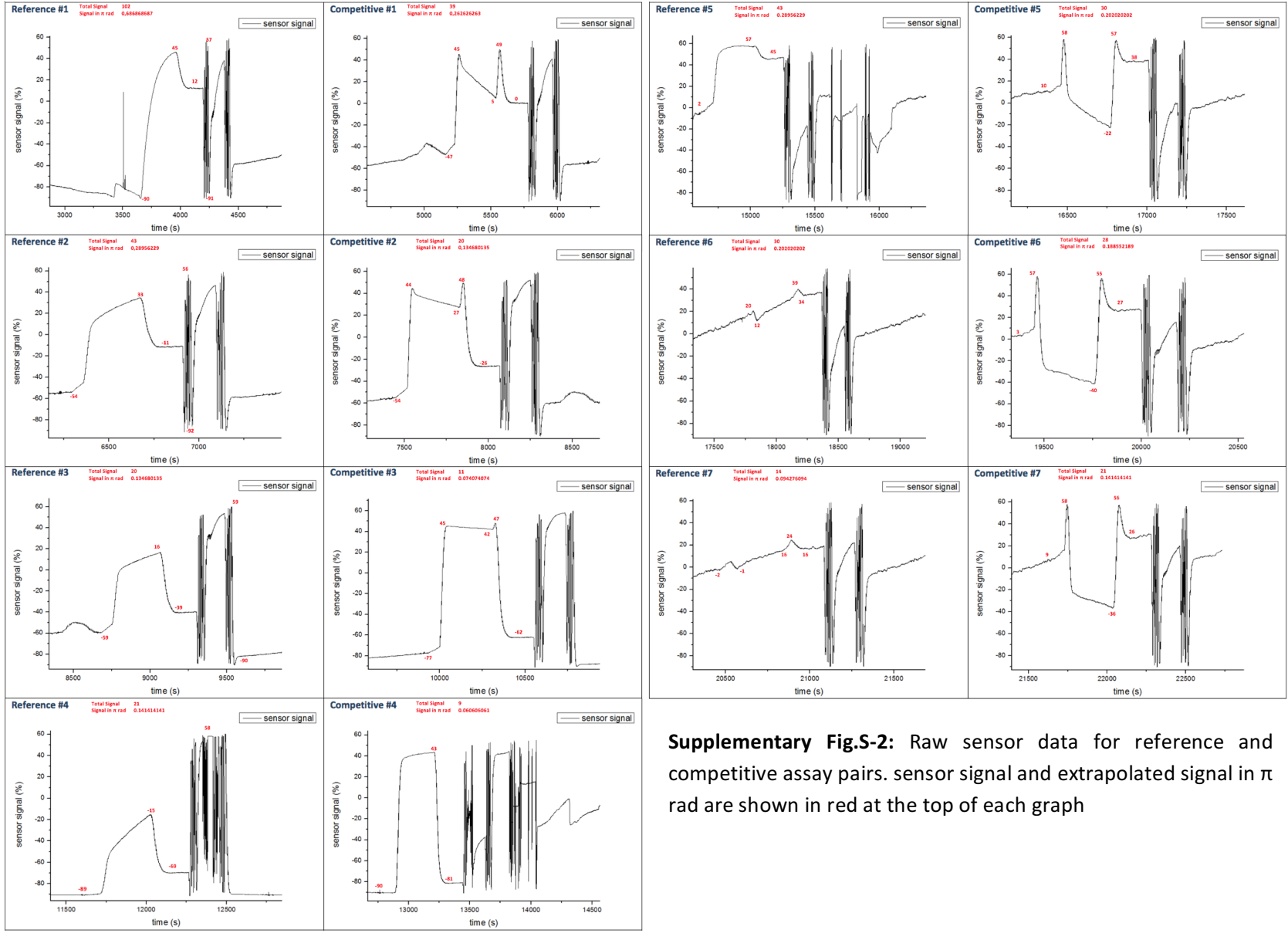
Operation of the Bimodal waveguide biosensor was conducted using an experimental setup similar to previously outlined¹. A He-Ne laser (632.8nm, 10 mW) was end-fire coupled to the biosensor through a 40x microscope objective using TE polarization, the resultant interferometric signal was acquired with a dual segment photodiode (S5870, Hamamatsu) and data analysis was performed using LabVIEW software (National Instruments, USA). The microfluidic module was clamped to the BiMW sensor directly between a PMMA clamp and a thermal regulation stage, stabilising intrinsic signal drift due to environmental thermal influence

Supplementary Fig.S-1: On chip diaphragm pump geometry



Supplementary Fig.S-1: On chip diaphragm pump geometry. Fig.S-1 A shows a dissected segment of the microfluidic module, showing the various critical components, and illustrating their relative size. A dashed line through the pump chamber shows a cut, with Fig.S-1 B showing a cross sectional image of this cut surface, illustrating the relative thickness of primary, membrane, and actuation chamber components of the valves used in this module.

Supplementary Fig.S-2: Raw sensor data



Supplementary Fig.S-2: Raw sensor data for reference and competitive assay pairs. sensor signal and extrapolated signal in π rad are shown in red at the top of each graph

REFERENCES

1. K. E. Zinoviev, A. B. González-Guerrero, C. Domínguez and L. M. Lechuga, *Journal of Lightwave Technology* **29** (13), 1926-1930 (2011).